A Superconducting Terahertz Flux-Flow Oscillator: Estimation of the Emission Power to Open Space

Nickolay V. Kinev
Laboratory of Superconducting Devices for Signal Detection and Processing
Kotelnikov Institute of Radio Engineering and Electronics of RAS
Moscow, Russia
nickolay@hitech.cplire.ru

Kirill I. Rudakov
Kapteyn Astronomical Institute
University of Groningen
Groningen, the Netherlands
rudakov@astro.rug.nl

Lyudmila V. Filippenko
Laboratory of Superconducting Devices for Signal Detection and Processing
Kotelnikov Institute of Radio Engineering and Electronics of RAS
Moscow, Russia
lyudmila@hitech.cplire.ru

Valery P. Koshelets
Laboratory of Superconducting Devices for Signal Detection and Processing
Kotelnikov Institute of Radio Engineering and Electronics of RAS
Moscow, Russia
valery@hitech.cplire.ru

2021 Radiation and Scattering of Electromagnetic Waves (RSEMW) | 978-1-6654-2544-5/21/$31.00 ©2021 IEEE | DOI: 10.1109/RSEMW52378.2021.9494096

***Abstract*—In this paper, we calculate power of electromagnetic wave emitted to open space by a terahertz (THz) source based on a Josephson flux-flow oscillator (FFO). The FFO is integrated with a transmitting slot antenna and a superconductor-insulator-superconductor (SIS) tunnel junction on a single chip, providing a frequency-tunable signal in a wide range of 200 – 700 GHz to open space. For non-calibrated power measurements, we used a highly sensitive silicon bolometer at 4.2 K. A small part of output FFO power is branched to the on-chip SIS-mixer and was estimated by absolute value by means of the Tien and Gordon photon-assisted tunneling theory. Using the absolute value, a calibrated power emitted to open space was estimated in the whole operating range. A power of from fractions to a few μW was obtained with a maximum of about 3 μW at 330 GHz.**

Keywords—terahertz oscillators, SIS junctions, silicon bolometer, emission power

I. Introduction

THz range is widely used nowadays in many field: radio astronomy and monitoring of atmosphere, material science and chemistry, research of living tissues in biology and medicine, as well as communication technologies and data processing such as THz imaging. THz spectroscopy is a great branch of technology applied for extremely wide range of tasks [1-3]. It is used for studies of carrier dynamics in semiconductors, superconductors and strongly correlated electron materials, conductivity processes [1]. Since THz emission is not destructive, it is utilized in biological systems to interrogate vibrational modes that extend across large portions of the biomolecular framework [4]. Another important task is noninvasive detecting of explosives and drugs in security systems [5].

Recently we developed an oscillator emitting to open space based on the superconducting FFO integrated with the on-chip transmitting slot antenna and the SIS harmonic mixer (HM) for frequency and phase locking [6-10]. We carefully studied its spectral properties [6,8,9], its operating range [7,9,10] which directly depends on properties of transmitting antenna, and demonstrated the FFO-based source operation for gas spectroscopy in laboratory conditions [11]. Nevertheless, the absolute power of THz emission to open space was not still defined accurately due to non-specified volt-watt sensitivity of bolometer in THz range. An estimation of on-chip power radiation is made, e.g., in [12] and about 1.3 μW at 0.76 THz was obtained, but the radiation was not provided to open space. In present work, we used a similar technique to evaluate the on-chip power detected by the SIS harmonic mixer, and then we estimated the power emitted to open space. For detecting the power to open space at non-calibrated mode, we used a silicon bolometer operating at liquid helium temperature.

The study is supported by the Russian Science Foundation (No. 17-79-20343). The experimental samples were fabricated using the Unique Science Unit (USU) No. 352529 at Kotelnikov Institute of Radio Engineering and Electronics of RAS, the operation of which is partially supported by the Russian Foundation for Basic Research (No. 19-52-80023).

II. Experimental Data

A. Oscillator Design and Experimental Setup

The FFO is based on a long SIS junction fabricated from Nb/AlO_x/Nb with dimensions of 700 × 16 μm for lower frequency band design (#1) and 400 × 16 μm for higher frequency band design (#2). The planar structure of the FFO-based microcircuit of design #2 is presented in Fig. 1 a. The distance between centers of slots of the antenna is 75 μm. An area of the HM is ~1.4 μm^2.

The FFO operation is discussed in detail in [6,7]. In brief, the frequency is defined by the dc voltage V_{DC} which is set by both bias current and control line current supplying a local magnetic field, and the power at certain frequency can be tuned widely by changing bias current. The operating frequency f is defined strictly by voltage according to Josephson constant of ~483.6 GHz/mV:

$$f = (2e/h)\, V_{DC}\,, \qquad (1)$$

where h is the Planck constant and e is the elementary charge.

The experimental setup for data measurements for further power evaluations is presented in Fig. 1 b, where the FFO-based microcircuits is shown schematically, so Fig. 1 a can be considered as an insert for Fig. 1 b. The FFO microchip is mounted on collecting semielliptical silicon lens and installed

978-1-6654-2544-5/21/$31.00 ©2021 IEEE

Authorized licensed use limited to: Kotel'nikov Inst of Radio Eng & Electronics - RAS. Downloaded on February 01,2022 at 16:12:59 UTC from IEEE Xplore. Restrictions apply.

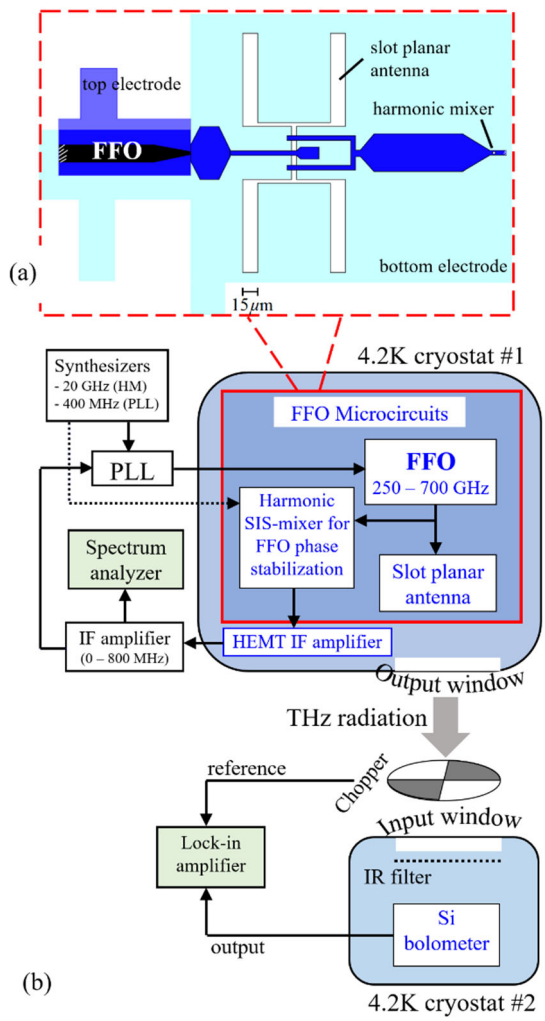

Fig. 1. (a) Layout of the microcircuit (design #2) containing the FFO, the double-slot antenna, the harmonic SIS mixer, and the coupling structures between the elements. (b) Block diagram of the experimental setup for detecting the emission to open space of the FFO-based subTHz/THz source in a wide frequency range.

in liquid helium cryostat (#1). The power measurements is carried out using the silicon bolometer in helium cryostat (#2) utilizing a common lock-in amplifier technique with chopping frequency of 170 Hz.

The experiment is carried out as follows. The FFO operating frequency is slowly sweeping in the operating V_{DC} range of ~0.4 – 1.6 mV corresponding to frequencies between 200 and 800 GHz, and also in the wide range of bias currents, while the bolometer response is measured. During the power measurements by bolometer, a pumping current of the HM is measured simultaneously. Additionally, *IV*-curve of the HM with pumping by FFO power at subTHz/THz frequency (so-called "pumped *IV*-curve") can be recorded at each operating frequency of interest. These *IV*-curves at specific frequencies are used in further calibrations.

B. Experimental Results

Primary experimental data for sample of design #1 obtained as described above (raw data) is presented in Fig. 2. For bolometer detection, the maximum response value at each operating frequency for different FFO bias currents is taken for final characteristics shown in Fig. 2 a. Results of numerical simulations are also shown by dotted curves; note

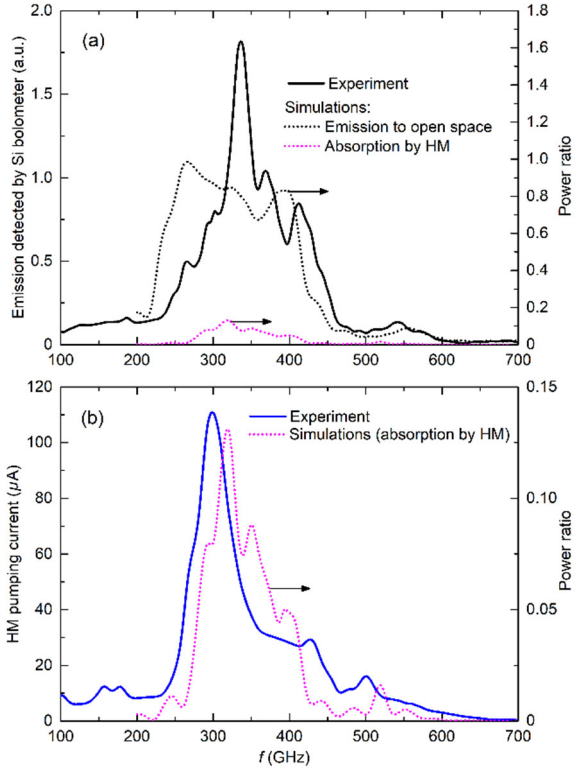

Fig. 2. (a) FFO emission to open space detected by Si bolometer (solid curve) and numerical simulations (dotted curves) for power normalized to the total output FFO power. (b) HM pumping (solid curve) and numerical simulation for absorption by HM (dotted curve), normalized to the total output FFO power.

that magenta curve for absorption by the HM is the same in both Figs. 2 (a) and (b) and presented in different scale.

One can note a sharp peak in power on experimental curve in Fig. 2 a at frequencies around 350 GHz, which is absent for simulation data. This can be explained by Fiske resonances and strongly different output FFO power at different operating points at resonant mode [13-14], while in simulations of the antenna-based structure the FFO power is considered to be constant. One can also note a rather good agreement of experiment and numerical data in Fig. 2 b with a small frequency shift of about 20 GHz. This shift can be easily explained by a minor technological deviation of an HM area from expected value of 1.4 μm^2 used in simulations. Nevertheless, such agreement between numerical and experimental results, though far from being perfect, allows us to make further power estimations assuming the known ratio between power emitted to open space and absorbed by the HM, which is taken from numerical simulations and is different at each frequency (i.e., ratio between dotted black and magenta curves in Fig. 2 a).

III. Techniques for Power Estimation and Results

A. Theory and Numerical Model

The quantum response of a nonlinear tunnel junction at high frequencies may be represented by an extension of the Tien and Gordon model of photon-assisted tunneling that is discussed in detail for SIS tunnel junctions in [15]. If an external signal of local oscillator at frequency ω is applied to the SIS junction, a time-dependent voltage across the junction occurs in addition to the dc bias:

$$V(t) = V_{DC} + V_{LO}\cos\omega t\ . \qquad (2)$$

Authorized licensed use limited to: Kotel'nikov Inst of Radio Eng & Electronics - RAS. Downloaded on February 01,2022 at 16:12:59 UTC from IEEE Xplore. Restrictions apply.

The resulting dc tunneling current will be given by the expression

$$I_{pump}(V_{DC},V_{LO}) = \sum_{n=-\infty}^{+\infty} J_n^2(\tfrac{eV_{LO}}{\hbar\omega}) I_{dc}(V_{DC} + n\tfrac{\hbar\omega}{e}), \quad (3)$$

where $I_{dc}(V)$ represents the autonomous (unmodulated) SIS *IV*-curve. The argument of the Bessel functions can be introduced by the dimensionless parameter α:

$$\alpha = eV_{LO} / \hbar\omega \; ; \quad (4)$$

the voltage corresponding to the width of the quasiparticle step on the SIS *IV*-curve is

$$V_S = \hbar\omega / e \; , \quad (5)$$

then (3) can be represented in a simpler form

$$I_{pump}(V_{DC},\alpha) = \sum_{n=-\infty}^{+\infty} J_n^2(\alpha) I_{dc}(V_{DC} + nV_S) . \quad (6)$$

The main task of numerical simulations is to define α at certain pumping frequency f using the experimental *IV*-curves, which were measured directly. Note that real FFO frequency f correspond to angular frequency ω used in (2)-(6) as $\omega = 2\pi f$. When α is known, the power absorbed by the HM is calculated as

$$P_{HM} = V_{LO}^{\,2} / R_\omega = \alpha^2 (\hbar\omega / e)^2 / R_\omega , \quad (7)$$

where R_ω is the resistance of the junction at a frequency of pumping defined as

$$R_\omega(V_{DC},\alpha) = \frac{2V_S}{I_{pump}(V_{DC}+V_S,\alpha) - I_{pump}(V_{DC}-V_S,\alpha)} \quad (8)$$

Once P_{HM} at certain frequency f is defined, the power emitted to open space P_{OS} is estimated directly using the known ratio P_{OS} / P_{HM} from high-frequency numerical simulations of the microcircuit design (see, e.g., dotted curves in Fig. 2 a). Then, since the absolute power emitted to open space is defined at specific frequency f, the whole "absolute power vs frequency" picture is recovered using the characteristics detected by the bolometer in a.u.

B. Results

To define α and estimate absolute power P_{HM} and P_{OS}, we developed a program for numerical simulations in MathCad® software, which calculates modulated *IV*-curves according to (6) and plots them on graph together with experimental *IV*-curves. Hence, choosing different α, the best fitting can be found as shown in Fig. 3 for two pumping frequencies of 296 GHz and 400 GHz, for the sample of design #1. Note that the critical current of the HM is not suppressed (black solid curve), while the unmodulated numerical *IV*-curve $I_{dc}(V)$ does not take into account the critical current (green dash-dotted curve). This leads to bad fitting on the quasiparticle step with number $n = -1$ due to additional Josephson steps on experimental curves which are absent on numerical curves.

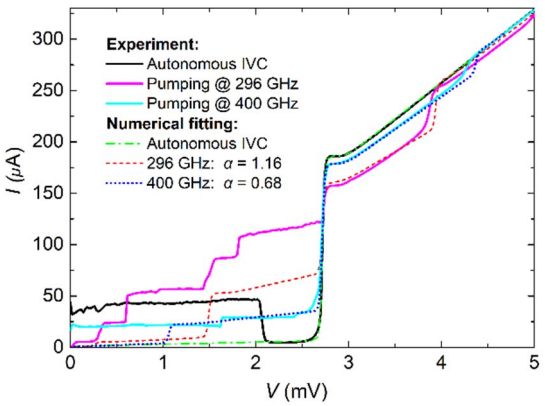

Fig. 3. Autonomous and pumped *IV*-curves of the HM, experimental (solid) and numerical (dashed-dotted and dotted) curves for the sample of design #1 at two frequencies.

Nevertheless, at voltages higher than gap voltage ~2.7 mV Josephson steps are not distinct, and rather good fitting for the step with number n = +1 can be found, as shown by red vs magenta and blue vs cyan curves, at 296 GHz and 400 GHz, correspondingly.

Specific calculations as an example are demonstrated below. First, it should be noted that maximum pumping current for the experimental sample under study is obtained at FFO frequency of 296 GHz, while in numerical simulations maximum is at 318.8 GHz (see Fig. 2 b). It is found that $\alpha = 1.16$ for pumping HM by FFO signal at 296 GHz according to Fig. 3. High-frequency resistance R_ω is calculated (8) to be ~12.67 Ω at this frequency, then allocated power is calculated (7) as $P_{HM} = 2.127 \cdot 10^{-7}$ W = 212.7 nW. At the same time, calculated ratio P_{OS} / P_{HM} is known at each frequency, and the point is that P_{OS} / P_{HM} at 318.8 GHz, but not at 296 GHz should be taken for calibration due to frequency shift of maximum pumping current. So, the ratio $P_{OS} / P_{HM} = 6.42$ is taken, then $P_{OS} = 1.366$ μW is obtained at 296 GHz using the ratio P_{OS} / P_{HM} at 318.8 GHz.

Results of calibrated power of emission to open space are presented in Fig. 4 for two designs #1 and #2 developed for the ranges of 250 – 420 GHz and 300 – 550 GHz. Points of calibration are marked by stars: 1.366 μW at 296 GHz for design #1 was described in detail above. The difference of emitted power obtained using different calibration points can

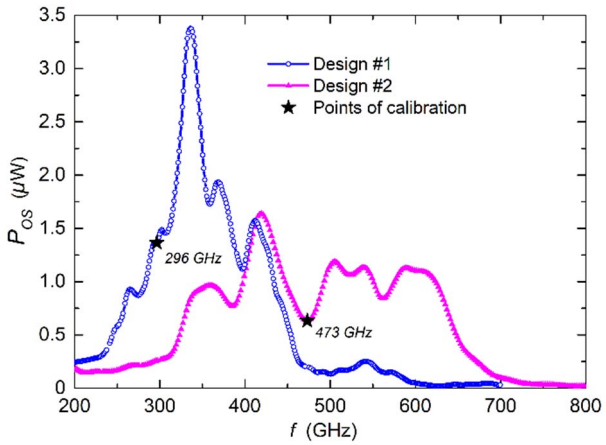

Fig. 4. Power of emission to open space of the FFO-based THz source detected by silicon bolometer and calibrated to absolute value using the photon-assisted pumping of the HM. Results for designs #1 and #2 developed for different frequency ranges, are presented.

Authorized licensed use limited to: Kotel'nikov Inst of Radio Eng & Electronics - RAS. Downloaded on February 01,2022 at 16:12:59 UTC from IEEE Xplore. Restrictions apply.

reach 50%, so the accuracy of out estimations is about 50%. However, this accuracy is enough to evaluate the order of the FFO power that can be emitted and detected in open space in the context of specific applications and developing the practical devices.

IV. Conclusions

A terahertz source based on the superconducting $Nb/AlO_x/Nb$ flux-flow oscillator is a promising solution for many fields where wideband frequency tuning is required and low temperature is not a principal problem. In this work, we studied the emission to open space of the FFO integrated with the on-chip transmitting antenna and the SIS junction commonly used as the harmonic mixer. The emission was studied by the external 4.2 K silicon bolometer located in separate cryostat.

Since the absolute power was unknown, we proposed and developed a technique to estimate the absolute power emitted to open space using the on-chip SIS mixer that is pumped by the FFO simultaneously. For this purpose, an extended model of Tien and Gordon was used, and the program for numerical calculations was developed. Two designs developed for different operating ranges of 250 – 420 GHz and 300 – 550 GHz were studied, and the emission power to open space from fractions to a few μW was estimated with a maximum of about 3 μW at 330 GHz. Such power value corresponds well to results in [12]. Though the power of a few μW is not high in comparison with other THz sources based, for example, on backward wave oscillators or Schottky diodes, it is sufficient for THz spectroscopy applications, for superconducting heterodyne receivers with high sensitivity, as well as for studying the properties of materials at low temperatures (~4.2 K) in the THz range. Moreover, it is better to use low-power sources in the case of high-sensitive detectors, to avoid saturation.

Acknowledgment

N.V.K. would like to acknowledge Fedor Khan for his help in software operation during simulations.

References

[1] S.L. Dexheimer, Terahertz Spectroscopy: Principles and Applications. CRC Press, New York, 2008, 360 p.

[2] M.C. Beard, G.M. Turner, and C.A. Schmuttenmaer, "Terahertz Spectroscopy," J. Phys. Chem. B, vol. 106, no. 29, pp. 7146–7159, Jun. 2002.

[3] J.B. Baxter and G.W. Guglietta, "Terahertz Spectroscopy," Anal. Chem., vol. 83, no. 12, pp. 4342–4368, May 2011.

[4] D.F. Plusquellic, K. Siegrist, E.J. Heilweil, and O. Esenturk, "Applications of Terahertz Spectroscopy in Biosystems," ChemPhysChem, vol. 8, no. 17, pp.2412–2431, Nov. 2007.

[5] A.G. Davies, A.D.Burnett, W. Fan, E.H. Linfield, and J.E. Cunningham, "Terahertz spectroscopy of explosives and drugs," Mater. Today, vol. 11, no. 3, pp. 18–26, Mar. 2008.

[6] N.V. Kinev, K.I. Rudakov, L.V. Filippenko, A.M. Baryshev, and V.P. Koshelets, "Flux-flow Josephson oscillator as the broadband tunable terahertz source to open space," J. Appl. Phys., vol. 125, no. 15, pp. 151603-1–151603-7, Mar. 2019.

[7] N.V. Kinev, K.I. Rudakov, L.V. Filippenko, A.M. Baryshev, and V.P. Koshelets, "Terahertz source radiating to open space based on the superconducting flux-flow oscillator: development and characterization," IEEE Trans. Terahertz Sci. Technol., vol. 9, no. 6, pp. 557–564, Sep. 2019.

[8] N.V. Kinev, K.I. Rudakov, L.V. Filippenko, A.M. Baryshev, and V.P. Koshelets, "An antenna with a feeder for a superconducting terahertz Josephson oscillator with phase locking," J. Commun. Technol. Electron., vol. 64, no. 10, pp. 1081–1086, Oct. 2019.

[9] N.V. Kinev, K.I. Rudakov, L.V. Filippenko, A.M. Baryshev, and V.P. Koshelets, "A Terahertz Source of Radiation to Open Space Based on a Long Josephson Junction," Phys. Solid State, vol.62, no. 9, pp. 1543 – 1548, Sep. 2020.

[10] N.V. Kinev, K.I. Rudakov, L.V. Filippenko, M.Yu. Fominskiy, A.M. Baryshev, and V.P. Koshelets, "A superconducting flux-flow oscillator of terahertz range," J. Physics Conf. Ser., vol. 1559, pp. 01221-1–01221-8, 2020.

[11] N.V. Kinev, K.I. Rudakov, L.V. Filippenko, A.M. Baryshev, and V.P. Koshelets, "Terahertz spectroscopy of gas absorption using the superconducting flux-flow oscillator as an active source and the superconducting integrated receiver," Sensors, vol. 20, no. 24, pp.7267-1–7267-16, Dec. 2020.

[12] S. Kohjiro, Z. Wang, S. V. Shitov, Sh. Miki, A. Kawakami, and A. Shoji, "Radiation Power of NbN-Based Flux-Flow Oscillators for THz-Band Integrated SIS Receivers," IEEE Trans. on Appl. Supercond., vol. 13, no. 2, pp.672–675, Jul. 2003.

[13] V.P. Koshelets, S.V. Shitov, A.V. Shchukin, L.V. Filippenko, J. Mygind, and A.V. Ustinov, "Self-Pumping Effects and Radiation Linewidth of Josephson Flux Flow Oscillator", Phys. Rev. B, vol. 56, no. 9, pp. 5572–5577, Sep. 1997.

[14] A.L. Pankratov, A.S. Sobolev, V.P. Koshelets, and J. Mygind, "Influence of surface losses and the self-pumping effect on current-voltage characteristics of a long Josephson junction," Phys. Rev. B, vol. 75, pp. 184516-1–184516-5, May 2007.

[15] J.R. Tucker and M.J. Feldman, "Quantum detection at millimeter wavelengths," Rev. Mod. Phys., vol. 57, no. 4, pp. 1055–1113, Oct. 1985.

Authorized licensed use limited to: Kotel'nikov Inst of Radio Eng & Electronics - RAS. Downloaded on February 01,2022 at 16:12:59 UTC from IEEE Xplore. Restrictions apply.